ACS APPLIED MATERIALS & INTERFACES

Research Article

www.acsami.org

White Upconversion Luminescence Nanocrystals for the Simultaneous and Selective Detection of 2,4,6-Trinitrotoluene and 2,4,6-Trinitrophenol

Yingxin Ma, Sheng Huang, Mingliang Deng, and Leyu Wang*

State Key Laboratory of Chemical Resource Engineering, Beijing Key Laboratory of Environmentally Harmful Chemical Analysis, Beijing University of Chemical Technology, Beijing 100029, China

Supporting Information

ABSTRACT: A highly water stable and strong upconversion (UC) luminescence $NaYF_4$@PSI−NH nanosensor for the simultaneous and selective detection of 2,4,6-trinitrotoluene (TNT) and 2,4,6-trinitrophenol (TNP) was successfully developed. Via the 980 nm near-infrared (NIR) irradiation, these nanosensors emit strong white UC luminescence with five typical emission peaks centered at 363, 455, 475, 546, and 654 nm. The UC emission at both 363 and 546 nm was quenched by the addition of TNT; however, the ratio of luminescence intensity at 363 nm to 546 nm (I_{363}/I_{546}) had no change with the increase of TNT concentration. Meanwhile, only violet UC emission at 363 nm was dramatically quenched via the addition of TNP, and the I_{363}/I_{546} ratio is negatively proportional to the TNP concentration in the range of 0.01−4.5 μg/mL of TNP. On the other hand, the green UC emission intensity at 546 nm is in negative proportion to the concentration of TNT. Moreover, cyclohexane, toluene, and other nitroaromatics (such as 2,4-dinitrotoluene (DNT) and nitrobenzene (NB)) have no influence on the detection. Therefore, we developed a facile method for the simultaneous and selective detection of TNT and TNP in the mixture solution of nitroaromatics independent of complicated instruments and sample pretreatment.

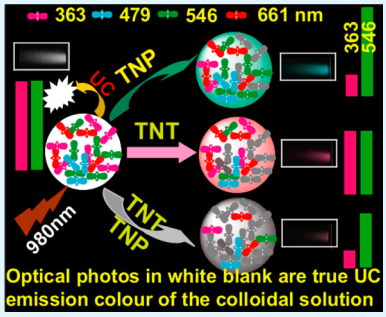

KEYWORDS: *nanoparticles, white upconversion luminescence, simultaneous detection, nitroaromatic explosives*

INTRODUCTION

Nitroaromatics, including 2,4,6-trinitrotoluene (TNT)[1] and 2,4,6-trinitrophenol (TNP),[2] are usually used as explosives in landmines for terrorist attack, military operation, and mines. Because of their biological persistence, toxicity, and mutagenicity, contamination of soil and groundwater with TNT and TNP has drawn widespread attention. Rapid, sensitive, and selective detection of TNT and TNP traces in aqueous environments has gained increasing concern, because these nitroaromatics are toxic to many organisms, ranging from plants to humans, and are closely related to homeland security and public safety.[3−10] Nitroaromatics such as 2,4-dinitrotoluene (DNT), nitrobenzene (NB), and especially TNP often interfere with the detection of TNT and give a false positive result.[2,11,12] To date, various methods including liquid chromatography−mass spectrometry (LC-MS), gas chromatography−mass spectrometry (GC-MS), solid-phase microextraction (SPME), high-performance liquid chromatography (HPLC), surface-enhanced Raman spectroscopy (SERS), and ion mobility spectrometry method have already been proposed to assay TNT.[4,5,13−18] However, these technologies rely mainly on complicated instruments and usually are time-consuming. In recent years, because of the novel property and simplicity, fluorescence-based sensors (especially quantum dots (QDs) and rare-earth doped nanomaterials) have drawn great attention and been extensively investigated for the selective and sensitive detection of TNT.[3,7,19−21] In order to enhance the selectivity of TNT detection, molecularly imprinted polymers (MIPs) and immunoassays were also developed for the analysis of TNT.[10,22,23] Despite the significant advantages that have been made for the detection of TNT, up to now, the differentiation of TNP and TNT is still a challenge because of their highly similar chemical structures and properties.[1,2] Therefore, it is still a challenge to develop a novel and facile strategy for the simultaneous and selective detection of TNT and TNP in the mixture nitroaromatic solution independent of expensive instruments and complicated sample pretreatment.

Herein, we developed a facile and rapid strategy for the simultaneous and selective detection of TNT and TNP in the mixed aqueous solution of nitroaromatics based on the white upconversion (UC) luminescence nanocrystals. As reported by Zhang,[12,15,24] TNT can dramatically quench the green luminescence after forming a TNT−amine complex. On the other hand, TNP has a very strong absorption of violet instead of green light, which can selectively quench the violet luminescence located at 365 nm.[2] By co-doping Yb^{3+}, Er^{3+}, and Tm^{3+} ions, $NaYF_4$ upconversion nanoparticles (UCNPs)[25−30] can emit strong white UC luminescence with

Received: February 20, 2014
Accepted: April 16, 2014
Published: April 16, 2014

   dx.doi.org/10.1021/am501053n | ACS Appl. Mater. Interfaces 2014, 6, 7790−7796

strong and sharp emission peaks at 349 nm (Tm^{3+}: $^1D_2 \rightarrow {}^3H_6$), 363 nm ($Tm^{3+}$: $^1D_2 \rightarrow {}^3H_6$; Er^{3+}: $^2G_{9/2} \rightarrow {}^4I_{15/2}$), 412 nm ($Er^{3+}$: $^4H_{9/2} \rightarrow {}^4I_{15/2}$), 455 nm ($Tm^{3+}$: $^1D_2 \rightarrow {}^3F_4$; Er^{3+}: $^4F_{5/2} \rightarrow {}^4I_{15/2}$), 479 nm ($Tm^{3+}$: $^1G_4 \rightarrow {}^3H_6$; Er^{3+}: $^4F_{7/2} \rightarrow {}^4I_{15/2}$), 546 nm ($Er^{3+}$: $^4S_{3/2} \rightarrow {}^4I_{15/2}$) and 661 nm ($Er^{3+}$: $^4F_{9/2} \rightarrow {}^4I_{15/2}$; Tm^{3+}: $^1G_4 \rightarrow {}^3F_4$), respectively (see Figure S1a in the Supporting Information).[31−40] In addition, the luminescence quantum yield of $NaYF_4$ UCNPs is usually in the range of 0.005%−0.3%.[41] It should be mentioned that, despite so many emission peaks, only the luminescence at 363 and 546 nm was investigated in this work. To make the formation of TNT−amine complex, the as-prepared hydrophobic UCNPs were successfully modified with oleylamine-conjugated polysuccinimide (PSI−NH)[42] and transferred into water via a modified strategy.

EXPERIMENTAL SECTION

Reagents and Chemicals. TNT and TNP were kindly supplied by National Security Department of China and recrystallized with ethanol before use. The white UC luminescence $NaYF_4$ nanocrystals and the oleylamine modification of polysuccinimide (PSI_{OAM}) were carried out according to our previous work.[1,42] $Y(NO_3)_3{\cdot}6H_2O$, $Er(NO_3)_3{\cdot}6H_2O$, and $Yb(NO_3)_3{\cdot}6H_2O$ (>99.9% purity) were purchased from Beijing Ouhe Chemical Reagent Company. All other reagents are analytical grade and used as received without further purification. DNT and NB were purchased from Aladdin Chemistry Co., Ltd. (China). The polysuccinimide (PSI)[1,42] was obtained from Shijiazhuang Desai Chemical Company and functionalized with oleylamine to form the amphiphilic PSI-NH. The oleic acid, sodium stearate, 1-octadecene, and oleylamine were purchased from Aldrich and used for the preparation of UCNPs. The stock solution of the four nitroaromatics was prepared by dissolving them into the mixed solvent of acetonitrile and ethanol (volume ratio = 1:4), respectively. NaOH, chloroform, ethanol, acetonitrile, cyclohexane, toluene, $NaHCO_3$, Na_2CO_3, NaAc, HAc, Na_2HPO_4, and NaH_2PO_4 were received from Beijing Chemical Factory (China).

Characterization. The shape and size of the UC $NaYF_4$ nanocrystals before and after coating with PSI_{OAM} were characterized by a Model H-800 transmission electron microscope (TEM) with a tungsten filament at an accelerating voltage of 100 kV. A Shimadzu Model XRD-7000 X-ray diffractometer, which employed Cu Kα radiation with a wavelength of λ = 1.5418 Å was used to record the X-ray diffraction (XRD) pattern. The infrared (IR) spectra were recorded on a Rigaku PLUS spectrometer (Tokyo). The absorption spectra were conducted on a UNICO Model 2802PC spectrophotometer with a spectral window range of 300−700 nm. The photoluminescence measurements were performed on a Model F-4600 spectrophotometer (Hitachi, Japan) with a 980-nm diode laser (Hi−Tech Optoelectronic Co. Ltd). Thermogravimetric analysis (TGA) was carried out via a simultaneous thermal analyzer (Model TGA/DSC 1/1100, SF Mettler−Toledo).

Surface Functionalization of UCNPs. The white UC luminescence $NaYF_4$ nanocrystals and the oleylamine modification of polysuccinimide (PSI_{OAM}) were carried out according to our previous work (see the Supporting Information).[1,32,42] Amine functionalization of the UCNPs was conducted via a facile microemulsion method.[43] Briefly, 1.0 mL of chloroform solution containing PSI−NH (54 mg) and $NaYF_4$:Yb^{3+}/Er^{3+}/Tm^{3+} UCNPs (2.25 mg) was added into 10 mL of NaOH (0.1 M) aqueous solution under ultrasonication and magnetic stirring. The hydrophilic nanocrystals were obtained and stored in deionized (DI) water for use after evaporating the chloroform. The final concentration of the colloidal solution was 5.1 mg/mL.

2,4,6-Trinitrotoluene (TNT) and 2,4,6-Trinitrophenol (TNP) Detection. Into each vial, 500 μL of the hydrophilic $NaYF_4$ UCNPs colloidal solution (5.1 mg/mL) was mixed with different amounts of nitroaromatics and 1.0 mL of product was obtained via the addition of NaOH−$NaHCO_3$ buffer solution (0.02 M, pH 12). The luminescence quenching effects were carried out with the irradiation of a 980-nm diode laser.

RESULTS AND DISCUSSION

As shown in Scheme 1, the imide-enriched UCNPs with white UC luminescence were used for the simultaneous and selective detection of TNT and TNP via the selective quenching of the UC luminescence. From Figure S1a in the Supporting Information, it is clear that these UCNPs can emit the white luminescence with multiple emission peaks at 349 nm (Tm^{3+}: $^1D_2 \rightarrow {}^3H_6$), 363 nm ($Tm^{3+}$: $^1D_2 \rightarrow {}^3H_6$; Er^{3+}: $^2G_{9/2} \rightarrow {}^4I_{15/2}$), 412 nm ($Er^{3+}$: $^4H_{9/2} \rightarrow {}^4I_{15/2}$), 455 nm ($Tm^{3+}$: $^1D_2 \rightarrow {}^3F_4$; Er^{3+}: $^4F_{5/2} \rightarrow {}^4I_{15/2}$), 479 nm ($Tm^{3+}$: $^1G_4 \rightarrow {}^3H_6$; Er^{3+}: $^4F_{7/2} \rightarrow {}^4I_{15/2}$), 546 ($Er^{3+}$: $^4S_{3/2} \rightarrow {}^4I_{15/2}$), and 661 ($Er^{3+}$: $^4F_{9/2} \rightarrow {}^4I_{15/2}$; Tm^{3+}: $^1G_4 \rightarrow {}^3F_4$) nm, respectively. Because of the absorption of TNP at 365 nm (Figure S1b in the Supporting Information), only the violet (363 nm) UC luminescence of the $NaYF_4$@PSI−NH UCNPs was dramatically quenched, and no influence on the green UC emission at 546 nm was observed. However, because of the wide absorption in the range of 350−600 nm by TNT (Figure S1b in the Supporting Information), the UC luminescence at both 363 and 546 nm was quenched gradually

Scheme 1. Scheme for the Simultaneous and Selective UC Luminescence Quenching Detection of TNT and TNP[a]

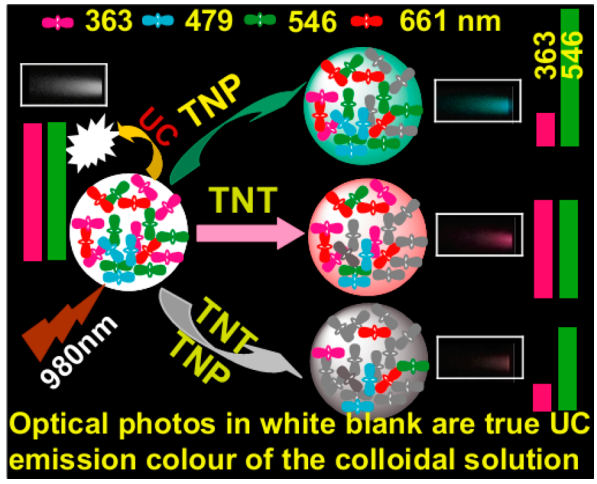

[a]The digital photos were obtained from the $NaYF_4$ NPs solution in the presence of different nitroaromatics (4.5 μg/mL) under the irradiation of a 980-nm diode laser. TNP quenched the 363 nm UC emission only; TNT quenched both 363 and 546 nm UC luminescence but the I_{363}/I_{546} ratio remained stable. In the presence of both TNP and TNT, the I_{363}/I_{546} ratio was negatively proportional to the concentration of TNP.

with the increase of TNT concentration, and the I_{363}/I_{546} ratio remained unchanged. Herein, the I_{363} and I_{546} represent the luminescence intensity at 363 and 546 nm, respectively. By adding the mixture solution of TNT and TNP, the UC emission at both 363 and 546 nm was decreased obviously and the I_{363}/I_{546} ratio was also decayed. Therefore, the linear decrease of the green UC luminescence at 546 nm can be used for the quantification of TNT, because TNP has no influence on this green emission. On the other hand, the TNT has no effects on the I_{363}/I_{546} ratio, and the proportional decay of this ratio is attributed to TNP. Thus, the ratio decay can be used for the quantitative detection of TNP. Moreover, other nitroaromatics (including 2,4-dinitrotoluene (DNT) and nitrobenzene (NB)) have no interference, because DNT and NB have no absorption in the range of 350−600 nm (see Figure S1b in the Supporting Information). The difference in the absorption spectra of TNT, TNP, DNT, and NB in the presence of $NaYF_4$@PSI−NH gives rise to the good selectivity of the as-developed method. Therefore, a novel upconversion luminescence nanosensor was successfully developed for the simultaneous and selective quantification of TNT and TNP in the aqueous solution of mixture nitroaromatics.

The morphology and size distribution of the $NaYF_4$ UCNPs was observed via transmission electron microscopy (TEM). From the TEM images shown in Figure 1, it is clear that the

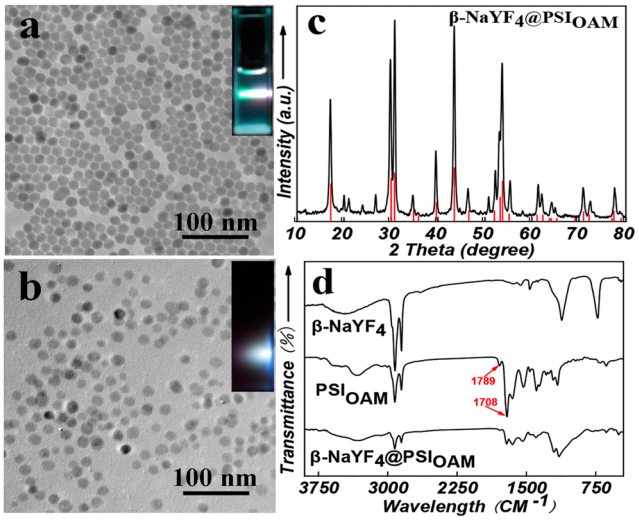

Figure 1. TEM images ((a) before and (b) after coating with PSI_{OAM}), (c) XRD spectra, and (d) FTIR spectra of the UCNPs.

particle size and shape of $NaYF_4$ have no obvious change before (Figure 1a) and after (Figure 1b) the surface functionalization. In addition, no aggregation can be observed from the surface functionalized UCNPs. As shown in the luminescence photos, compared to the hydrophobic UCNPs dispersed in chloroform (see inset of Figure 1a), the white UC luminescence of the $NaYF_4$@PSI−NH UCNPs dispersed in water was well-retained (see inset of Figure 1b). In addition, the chemical composition and crystallinity of the UC nanocrystals were further checked via X-ray diffraction (XRD) and the results suggest that the NPs are hexagonal-phase $NaYF_4$ with good crystallinity (Figure 1c). Moreover, the PSI−NH coating was identified through the Fourier transform infrared spectroscopy (FTIR) spectra (Figure 1d). The characteristic peaks of lactam rings of PSI at ~1789 and 1708 cm^{-1} for C═O and the carboxylic group at ~1712 cm^{-1} cannot be observed from the spectrum of the as-prepared hydrophobic $NaYF_4$. However, the vibration adsorption peaks of lactam rings[42] were observed on PSI−NH and weaken on the $NaYF_4$@PSI−NH UCNPs, because most of the lactam rings were hydrolyzed to carboxylic groups during the nanoparticle surface modification, in agreement with the peak of 1712 cm^{-1} in the spectrum of $NaYF_4$@PSI−NH. Other characteristic peaks in the spectrum of $NaYF_4$@PSI−NH are in accordance with those in the spectrum of PSI−NH, further suggesting PSI−NH coating is successful. The PSI coating is further characterized with the TGA results. As shown in Figure S2, the weight loss of the PSI coated UCNPs is about 30% when the temperature is increased to 500 °C, and no further weight loss is observed by increasing the temperature up to 800 °C.

To investigate the feasibility of using these UCNPs as luminescent sensors for the simultaneous and selective detection of TNT and TNP, the luminescence quenching by TNT and TNP was checked at different pH values. As shown in Figure 2, in the absence of TNP, the luminescence at both 363

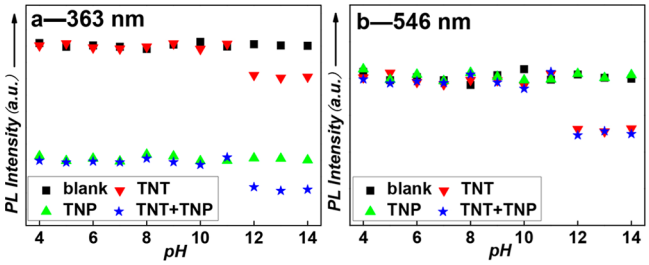

Figure 2. pH influence on the UC luminescence intensity of the UCNPs (2.55 mg/mL) at (a) 363 nm and (b) 546 nm. Buffer solution and concentration: pH (4, 5), CH_3COOH−CH_3COONa (0.02 M); pH (6−8), NaH_2PO_4−Na_2HPO_4 (0.02 M): pH (9−14), NaOH−Na_2CO_3−$NaHCO_3$ (0.02 M). Nitroaromatic solution and concentration: TNT, 2.0 μg/mL; TNP, 2 μg/mL; TNT + TNP, 2 μg/mL + 2 μg/mL.

and 546 nm was almost unaffected by pH values. After the addition of TNP, the luminescence of 363 nm was dramatically quenched, but the quenching degree was not influenced by pH values. Meanwhile, the TNP has no effects on the green UC emission at 546 nm over the entire pH range of 4−14. Different from TNP, the TNT has no influence on the 365 and 546 nm luminescence in the range of pH 4−11. However, under strong basic conditions (pH 12−14), the luminescence at both 365 and 546 nm was obviously quenched and the degree of luminescence quenching was same in this pH range (12−14). It can be attributed to the deprotonation of the methyl group of TNT by the amide to form the colored TNT anion (see Scheme S1 in the Supporting Information) that can absorb the UC luminescence.[12,15] In the current work, the simultaneous and selective analysis of TNT and TNP was conducted at pH 12.

As a sensor for the simultaneously selective and sensitive detection of TNT and TNP in the mixture solution, rapid response to the target nitroaromatic is in high demand. Therefore, the influence of incubation time on the luminescence intensity was also investigated. As shown in Figure 3 (a1 and a2), the luminescence at both 363 and 546 nm was quenched instantly with the addition of TNT at pH 12. Meanwhile, by prolonging the incubation time to 4 h, the luminescence intensity was almost unchanged and the I_{363}/I_{546} ratio had a slight fluctuation over the entire time range. In the

dx.doi.org/10.1021/am501053n | ACS Appl. Mater. Interfaces 2014, 6, 7790−7796

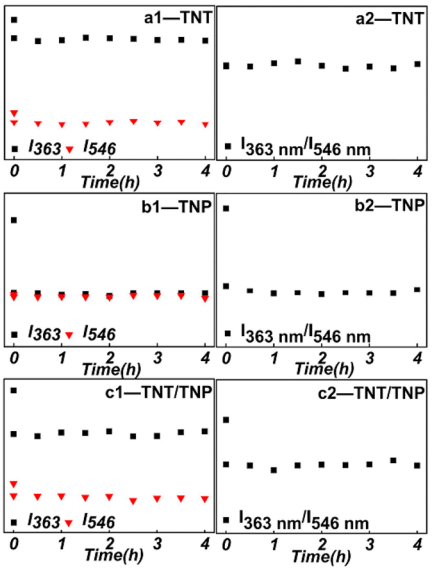

Figure 3. Effects of incubation time on the UC luminescence at 363 nm, 546 nm, and the I_{363}/I_{546} ratio in the presence of (a1 and a2) TNT (2.0 μg/mL), (b1 and b2) TNP (2.0 μg/mL), and (c1 and c2) TNT (2.0 μg/mL) + TNP (2.0 μg/mL). UCNPs: 2.55 mg/mL.

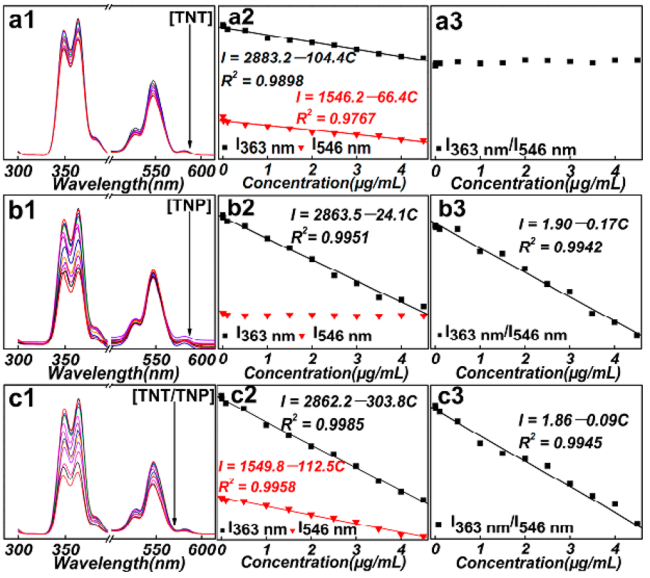

Figure 4. Luminescence evolution of the hydrophilic $NaYF_4$ UCNPs (2.55 mg/mL) colloidal solution in the presence of various concentration of (a1) TNT, (b1) TNP, and (c1) TNT/TNP; also shown are corresponding calibration curves of UC luminescence intensity at 363 and 546 nm versus explosive concentration for (a2) TNT, (b2) TNP, and (c2) TNT/TNP, and calibration curves of the I_{363}/I_{546} ratio versus the concentration of (a3) TNT, (b3) TNP, and (c3) TNT/TNP.

case of TNP, the luminescence intensity at 363 nm was quenched dramatically as soon as the TNP was added and remained stable during the rest of the 4 h. Meanwhile, the green luminescence at 546 nm was not quenched (Figure 3b1), and the I_{363}/I_{546} ratio had a change similar to that of I_{363} (see Figure 3b2). As depicted in Figures 3c1 and 3c2, by adding the mixture of TNT and TNP into the UCNPs colloidal solution, the values of I_{363}, I_{546}, and I_{363}/I_{546} decreased instantly and remained stable during the rest of incubation time, respectively. These phenomena demonstrate that the UCNPs-based luminescence detection method is very rapid, and stable over a long period of time.

As shown in Figure 4a, the relative luminescence intensity of hydrophilic $NaYF_4$ NPs at 363 nm and 546 nm decayed linearly with the increase of the TNT concentration in the range of 0.01−4.5 μg/mL (see Figures 4a1 and 4a2) and the I_{363}/I_{546} ratio remained stable with the addition of TNT (Figure 4a3). Meanwhile, the luminescence spectra of the UCNPs also demonstrated that the luminescence intensity decreased step by step at both 363 and 546 nm by increasing the concentration of TNT at pH 12. In the case of TNP, the UC luminescence intensity at 363 nm was quenched dramatically and proportionally with the increase of TNP concentration in the range of 0.01−4.5 μg/mL. The luminescence at 546 nm, however, was hardly influenced (see Figures 4b1 and 4b2). Therefore, the I_{363}/I_{546} ratio versus the TNP concentration plot has a decay trend similar to that of the luminescence at 363 nm (see Figure 4b3). We then checked the evolution of luminescence intensity by adding a series concentration of the mixed solution of TNT and TNP, and the results are shown in Figure 4c. By increasing the concentration of TNT and TNP, the relative luminescence intensity at 363 and 546 nm, and the I_{363}/I_{546} ratio were all decayed linearly to the concentration of nitroaromatics in the range of 0.01−4.5 μg/mL. A calibration function of I_{546} = 1547.5 − 66.1C (n = 12) with good linearity (R^2 = 0.9754) for the TNT analysis in the mixed solution of TNT and TNP was obtained (Figure 4c2). Meanwhile, the decrease in the I_{363}/I_{546} ratio was attributed to the presence of TNP and the good linearity (R^2 = 0.9955) with a calibration function of I_{363}/I_{546} = 1.87 − 0.15C (n = 12) can be used for the quantitative detection of TNP (Figure 4c3). Moreover, the 3σ limits of detection for TNT and TNP were 8.4 and 9.6 ng/mL, respectively. Herein, C is the concentration of nitroaromatics (μg/mL), and n is the number of datum points on the line.

To illustrate the good selectivity of this newly developed method, effects of DNT and NB on the UC luminescence were further investigated and the results are shown in Figure 5. After

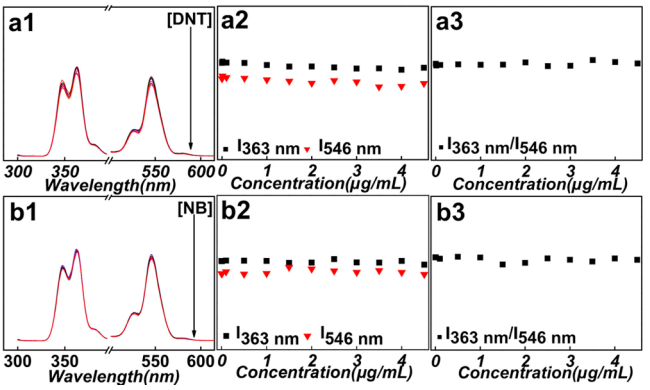

Figure 5. Effects of (a1−a3) DNT and (b1−b3) NB on the UC luminescence at 363 and 546 nm. UCNPs (2.55 mg/mL).

adding a given concentration of DNT or NB into the solution of hydrophilic $NaYF_4$ UCNPs colloidal solution, the UC luminescence spectra were carried out with the irradiation of a 980-nm diode laser. As shown in Figure 5, the relative UC luminescence intensity at 363 and 546 nm, and the I_{363}/I_{546} ratio, were all unchanged in the range of 0.01−4.5 μg/mL of DNT or NB. The results suggest that DNT and NB have no influence on the TNT and TNP analysis. The influence of

dx.doi.org/10.1021/am501053n | ACS Appl. Mater. Interfaces 2014, 6, 7790−7796

cyclohexane and toluene was also investigated and no effects on the detection of TNT and TNP were observed (see Figure S3 in the Supporting Information). The optical photos of the UCNPs colloidal solution in the presence of different amount of TNT or TNP also have been shown in Figure S4 in the Supporting Information. The selectivity and applicability of this method was further proved through the analysis results on the mixed samples of these four nitroaromatics (Table S1 in the Supporting Information). All of these results demonstrate that a novel method has been successfully developed for simultaneous selective and sensitive luminescence detection of TNT and TNP in a mixed solution of nitroaromatics.

To further note the advantages of our work, we compared this strategy with other publications on UCNPs luminescence detection of nitroaromatics in Table 1 and with recent papers for detection of nitroaromatics by other methods in Table 2. The comparison suggests that the developed method truly own its advantage for the simultaneous and selective detection of TNT and TNP in mixture aqueous samples.

Table 1. Comparison of Nanosensor Based on the White UCNPs and Other UCNPs

method	linear range (TNT)	3σ (TNT)	selectivity
white-UCNPs	0.01−4.5 μg/mL	8.4 ng/mL	can differentiate and detect TNP
ref 1	0−8.0 μg/mL	N/A[a]	can differentiate but cannot detect TNP
ref 21	0.01−9.0 μg/mL	9.7 ng/mL	can differentiate but cannot detect TNP

[a]Not available.

CONCLUSION

In brief, we have developed a facile and rapid method to fabricate the hydrophilic $NaYF_4$ UCNPs with white upconversion (UC) luminescence by means of PSI_{OAM} coating. Because of the strong charge-transfer complexing interaction between TNT and PSI_{OAM}, the anionic form of TNT can absorb the luminescence at both 363 and 546 nm, and the I_{363}/I_{546} ratio is kept stable. As the TNP concentration progressively increased, only the luminescence intensity at 363 nm decreased and the I_{363}/I_{546} decay was attributed to the addition of TNP. So, we can quantitatively detect TNT via the calibration function of the luminescence intensity at 546 nm versus the concentration of TNT. Meanwhile, the calibration function of the I_{363}/I_{546} ratio versus the concentration of TNP can be used for the quantification of TNP. Therefore, based on the novel UCNPs, a facile and rapid method has been successfully developed for the simultaneous, selective, and sensitive detection of TNT and TNP from the mixture solution of nitroaromatics, independent of complicated instruments, immunoassays, or molecularly imprinted technologies.

ASSOCIATED CONTENT

Supporting Information

Synthesis of UCNPs, preparation of PSI_{OAm}, scheme for the charge-transfer interaction, UC emission spectrum, absorption spectra, effects of cyclohexane and toluene on UCNPs luminescence, the digital photos of the UCNPs, TGA of the UCNPs@PSI_{OAM}, detection of TNT and TNP in mixed water samples and real water samples. This material is available free of charge via the Internet at http://pubs.acs.org.

AUTHOR INFORMATION

Corresponding Author

*Tel./Fax: 0086-10-64427869. E-mail: lywang@mail.buct.edu.cn.

Notes

The authors declare no competing financial interest.

ACKNOWLEDGMENTS

We thank the financial support from the National Natural Science Foundation of China (No. 21275015) and the State Key Project of Fundamental Research of China (Nos. 2011CBA00503 and 2011CB932403). We are also grateful for the Program for New Century Excellent Talents in University of China (No. NCET100213) and the Science Foundation of Xinjiang Uygur Autonomous Region (No. 201191170). We also would like to thank the Scientific Research Foundation for the Returned Overseas Chinese Scholars (State Education Ministry), the Program for Changjiang Scholars and Innovative Research Team in University (No. IRT1205), and the Foundational Research Funds for the Central University (No. ZZ1321).We acknowledge the support from the "Public Hatching Platform for Recruited Talents of Beijing University of Chemical Technology".

REFERENCES

(1) Tu, N. N.; Wang, L. Y. Surface Plasmon Resonance Enhanced Upconversion Luminescence in Aqueous Media for TNT Selective Detection. *Chem. Commun.* **2013**, *49*, 6319−6321.

(2) Ma, Y. X.; Li, H.; Peng, S.; Wang, L. Y. Highly Selective and Sensitive Fluorescent Paper Sensor for Nitroaromatic Explosive Detection. *Anal. Chem.* **2012**, *84*, 8415−8421.

(3) Zhang, K.; Zhou, H. B.; Mei, Q. S.; Wang, S. H.; Guan, G. J.; Liu, R. Y.; Zhang, J.; Zhang, Z. P. Instant Visual Detection of Trinitrotoluene Particulates on Various Surfaces by Ratiometric Fluorescence of Dual-Emission Quantum Dots Hybrid. *J. Am. Chem. Soc.* **2011**, *133*, 8424−8427.

Table 2. Comparison of White UCNPs Nanosensor and Reported Methods

	TNT Detection		TNP Detection		
method	linear range	3σ	linear range	3σ	differentiate TNT and TNP
white-UCNPs	0.01−4.5 μg/mL	8.4 ng/mL	0.01−4.5 μg/mL	9.6 ng/mL	yes
ref 44	10^{-3}−10^{-8} M	66 μM	N/A[a]	N/A[a]	no
ref 45	N/A[a]a	N/A[a]	N/A[a]	22 nM	yes
ref 46	N/A[a]	N/A[a]	2×10^{-3}−1×10^{-14} M	N/A[a]	yes
ref 47	0.8−30 μM	0.28 μM	N/A[a]	N/A[a]	no

[a]Not available.

(4) Dasary, S. S. R.; Singh, A. K.; Senapati, D.; Yu, H. T.; Ray, P. C. Gold Nanoparticle Based Label-Free SERS Probe for Ultrasensitive and Selective Detection of Trinitrotoluene. *J. Am. Chem. Soc.* **2009**, *131*, 13806−13812.
(5) Engel, Y.; Elnathan, R.; Pevzner, A.; Davidi, G.; Flaxer, E.; Patolsky, F. Supersensitive Detection of Explosives by Silicon Nanowire Arrays. *Angew. Chem.—Int. Ed.* **2010**, *49*, 6830−6835.
(6) Anderson, G. P.; Goldman, E. R. TNT Detection Using Llama Antibodies and a Two-Step Competitive Fluid Array Immunoassay. *J. Immunol. Methods* **2008**, *339*, 47−54.
(7) Nie, H. R.; Zhao, Y.; Zhang, M.; Ma, Y. G.; Baumgarten, M.; Mullen, K. Detection of TNT Explosives with a New Fluorescent Conjugated Polycarbazole Polymer. *Chem. Commun.* **2011**, *47*, 1234−1236.
(8) Chen, H. W.; Hu, B.; Hu, Y.; Huan, Y. F.; Zhou, Z. Q.; Qiao, X. F. Neutral Desorption Using a Sealed Enclosure to Sample Explosives on Human Skin for Rapid Detection by EESI-MS. *J. Am. Soc. Mass Spectrosc.* **2009**, *20*, 719−722.
(9) Sohn, H.; Sailor, M. J.; Magde, D.; Trogler, W. C. Detection of Nitroaromatic Explosives Based on Photoluminescent Polymers Containing Metalloles. *J. Am. Chem. Soc.* **2003**, *125*, 3821−3830.
(10) Li, J.; Kendig, C. E.; Nesterov, E. E. Chemosensory Performance of Molecularly Imprinted Fluorescent Conjugated Polymer Materials. *J. Am. Chem. Soc.* **2007**, *129*, 15911−15918.
(11) Cerruti, M.; Jaworski, J.; Raorane, D.; Zueger, C.; Varadarajan, J.; Carraro, C.; Lee, S. W.; Maboudian, R.; Majumdar, A. Polymer-Oligopeptide Composite Coating for Selective Detection of Explosives in Water. *Anal. Chem.* **2009**, *81*, 4192−4199.
(12) Gao, D. M.; Wang, Z. Y.; Liu, B. H.; Ni, L.; Wu, M. H.; Zhang, Z. P. Resonance Energy Transfer-Amplifying Fluorescence Quenching at the Surface of Silica Nanoparticles toward Ultrasensitive Detection of TNT. *Anal. Chem.* **2008**, *80*, 8545−8553.
(13) Berg, M.; Bolotin, J.; Hofstetter, T. B. Compound-Specific Nitrogen and Carbon Isotope Analysis of Nitroaromatic Compounds in Aqueous Samples Using Solid-phase Microextraction Coupled to GC/IRMS. *Anal Chem.* **2007**, *79*, 2386−2393.
(14) Honeychurch, K. C.; Hart, J. P.; Pritchard, P. R. J.; Hawkins, S. J.; Ratcliffe, N. M. Development of an Electrochemical Assay for 2,6-Dinitrotoluene, Based on a Screen-Printed Carbon Electrode, and its Potential Application in Bioanalysis, Occupational and Public Health. *Biosens. Bioelectron.* **2003**, *19*, 305−312.
(15) Zhou, H. B.; Zhang, Z. P.; Jiang, C. L.; Guan, G. J.; Zhang, K.; Mei, Q. S.; Liu, R. Y.; Wang, S. H. Trinitrotoluene Explosive Lights up Ultrahigh Raman Scattering of Nonresonant Molecule on a Top-Closed Silver Nanotube Array. *Anal. Chem.* **2011**, *83*, 6913−6917.
(16) Guerra-Diaz, P.; Gura, S.; Almirall, J. R. Dynamic Planar Solid Phase Microextraction-Ion Mobility Spectrometry for Rapid Field Air Sampling and Analysis of Illicit Drugs and Explosives. *Anal. Chem.* **2010**, *82*, 2826−2835.
(17) Sanchez, C.; Carlsson, H.; Colmsjo, A.; Crescenzi, C.; Batlle, R. Determination of Nitroaromatic Compounds in Air Samples at Femtogram Level Using C-18 Membrane Sampling and on-Line Extraction with LC-MS. *Anal. Chem.* **2003**, *75*, 4639−4645.
(18) Moros, J.; Lorenzo, J. A.; Lucena, P.; Tobaria, L. M.; Laserna, J. J. Simultaneous Raman Spectroscopy-Laser-induced Breakdown Spectroscopy for Instant Standoff Analysis of Explosives Using a Mobile Integrated Sensor Platform. *Anal. Chem.* **2010**, *82*, 1389−1400.
(19) Tu, R. Y.; Liu, B. H.; Wang, Z. Y.; Gao, D. M.; Wang, F.; Fang, Q. L.; Zhang, Z. P. Amine-Capped ZnS-Mn^{2+} Nanocrystals for Fluorescence Detection of Trace TNT Explosive. *Anal. Chem.* **2008**, *80*, 3458−3465.
(20) Olley, D. A.; Wren, E. J.; Vamvounis, G.; Fernee, M. J.; Wang, X.; Burn, P. L.; Meredith, P.; Shaw, P. E. Explosive Sensing with Fluorescent Dendrimers: The Role of Collisional Quenching. *Chem. Mater.* **2011**, *23*, 789−794.
(21) Ma, Y.; Wang, L. UpconversionLuminescence Nanosensor for TNT Selective and Label-Free Quantification in the Mixture of Nitroaromatic Explosives. *Talanta* **2014**, *120*, 100−105.
(22) Xie, C. G.; Liu, B. H.; Wang, Z. Y.; Gao, D. M.; Guan, G. J.; Zhang, Z. P. Molecular Imprinting at Walls of Silica Nanotubes for TNT Recognition. *Anal. Chem.* **2008**, *80*, 437−443.
(23) Goldman, E. R.; Medintz, I. L.; Whitley, J. L.; Hayhurst, A.; Clapp, A. R.; Uyeda, H. T.; Deschamps, J. R.; Lassman, M. E.; Mattoussi, H. A Hybrid Quantum Dot-Antibody Fragment Fluorescence Resonance Energy Transfer-Based TNT Sensor. *J. Am. Chem. Soc.* **2005**, *127*, 6744−6751.
(24) Fang, Q. L.; Geng, J. L.; Liu, B. H.; Gao, D. M.; Li, F.; Wang, Z. Y.; Guan, G. J.; Zhang, Z. P. Inverted Opal Fluorescent Film Chemosensor for the Detection of Explosive Nitroaromatic Vapors Through Fluorescence Resonance Energy Transfer. *Chem.—Eur. J.* **2009**, *15*, 11507−11514.
(25) Chen, G. Y.; Ohulchanskyy, T. Y.; Kumar, R.; Agren, H.; Prasad, P. N. Ultrasmall Monodisperse $NaYF_4$:Yb^{3+}/Tm^{3+} Nanocrystals with Enhanced Near-Infrared to Near-Infrared Upconversion Photoluminescence. *ACS Nano* **2010**, *4*, 3163−3168.
(26) Dai, Y. L.; Ma, P. A.; Cheng, Z. Y.; Kang, X. J.; Zhang, X.; Hou, Z. Y.; Li, C. X.; Yang, D. M.; Zhai, X. F.; Lin, J. Up-Conversion Cell Imaging and pH-Induced Thermally Controlled Drug Release from $NaYF_4$:Yb^{3+}/Er^{3+}@Hydrogel Core-Shell Hybrid Microspheres. *ACS Nano* **2012**, *6*, 3327−3338.
(27) Saboktakin, M.; Ye, X. C.; Oh, S. J.; Hong, S. H.; Fafarman, A. T.; Chettiar, U. K.; Engheta, N.; Murray, C. B.; Kagan, C. R. Metal-Enhanced Upconversion Luminescence Tunable through Metal Nanoparticle−Nanophosphor Separation. *ACS Nano* **2012**, *6*, 8758−8766.
(28) Vetrone, F.; Naccache, R.; Zamarron, A.; de la Fuente, A. J.; Sanz-Rodriguez, F.; Maestro, L. M.; Rodriguez, E. M.; Jaque, D.; Sole, J. G.; Capobianco, J. A. Temperature Sensing Using Fluorescent Nanothermometers. *ACS Nano* **2010**, *4*, 3254−3258.
(29) Zhang, W. H.; Ding, F.; Chou, S. Y. Large Enhancement of Upconversion Luminescence of $NaYF_4$:Yb^{3+}/Er^{3+} Nanocrystal by 3D Plasmonic Nano-Antennas. *Adv. Mater.* **2012**, *24*, OP236−OP241.
(30) Johnson, N. J. J.; Korinek, A.; Dong, C. H.; van Veggel, F. Self-Focusing by Ostwald Ripening: A Strategy for Layer-by-Layer Epitaxial Growth on Upconverting Nanocrystals. *J. Am. Chem. Soc.* **2012**, *134*, 11068−11071.
(31) Chan, E. M.; Gargas, D. J.; Schuck, P. J.; Milliron, D. J. Concentrating and Recycling Energy in Lanthanide Codopants for Efficient and Spectrally Pure Emission: The Case of $NaYF_4$:Er^{3+}/Tm^{3+} Upconverting Nanocrystals. *J. Phys. Chem. B* **2012**, *116*, 10561−10570.
(32) Deng, M. L.; Ma, Y. X.; Huang, S.; Hu, G. F.; Wang, L. Y. Monodisperse Upconversion $NaYF_4$ Nanocrystals: Syntheses and Bioapplications. *Nano Res.* **2011**, *4*, 685−694.
(33) Boyer, J. C.; Vetrone, F.; Cuccia, L. A.; Capobianco, J. A. Synthesis of Colloidal Upconverting $NaYF_4$ Nanocrystals Doped with Er^{3+}, Yb^{3+} and Tm^{3+}, Yb^{3+} Via Thermal Decomposition of Lanthanide Trifluoroacetate Precursors. *J. Am. Chem. Soc.* **2006**, *128*, 7444−7445.
(34) Liu, Q.; Sun, Y.; Yang, T. S.; Feng, W.; Li, C. G.; Li, F. Y. Sub-10 nm Hexagonal Lanthanide-Doped $NaLuF_4$ Upconversion Nanocrystals for Sensitive Bioimaging in Vivo. *J. Am. Chem. Soc.* **2011**, *133*, 17122−17125.
(35) Wang, F.; Liu, X. G. Upconversion Multicolor Fine-Tuning: Visible to Near-Infrared Emission from Lanthanide-Doped $NaYF_4$ Nanoparticles. *J. Am. Chem. Soc.* **2008**, *130*, 5642−5643.
(36) Wang, J. W.; Tanner, P. A. Upconversion for White Light Generation by a Single Compound. *J. Am. Chem. Soc.* **2010**, *132*, 947−949.
(37) Li, L. L.; Zhang, R. B.; Yin, L. L.; Zheng, K. Z.; Qin, W. P.; Selvin, P. R.; Lu, Y. Biomimetic Surface Engineering of Lanthanide-Doped Upconversion Nanoparticles as Versatile Bioprobes. *Angew. Chem.—Int. Ed.* **2012**, *51*, 6121−6125.
(38) Tu, D. T.; Liu, Y. S.; Zhu, H. M.; Li, R. F.; Liu, L. Q.; Chen, X. Y. Breakdown of Crystallographic Site Symmetry in Lanthanide-Doped $NaYF_4$ Crystals. *Angew. Chem.—Int. Ed.* **2013**, *52*, 1128−1133.
(39) Yang, Y. M.; Shao, Q.; Deng, R. R.; Wang, C.; Teng, X.; Cheng, K.; Cheng, Z.; Huang, L.; Liu, Z.; Liu, X. G.; Xing, B. G. In Vitro and In Vivo Uncaging and Bioluminescence Imaging by Using Photocaged

Upconversion Nanoparticles. *Angew. Chem.—Int. Ed.* **2012**, *51*, 3125−3129.
(40) Zhang, H.; Li, Y. J.; Ivanov, I. A.; Qu, Y. Q.; Huang, Y.; Duan, X. F. Plasmonic Modulation of the Upconversion Fluorescence in $NaYF_4$:Yb/Tm Hexaplate Nanocrystals Using Gold Nanoparticles or Nanoshells. *Angew. Chem.—Int. Ed.* **2010**, *49*, 2865−2868.
(41) Boyer, J. C.; van Veggel, F. C. J. M. Absolute Quantum Yield Measurements of Colloidal $NaYF_4$: Er^{3+}, Yb^{3+} Upconverting Nanoparticles. *Nanoscale* **2010**, *2*, 1417−1419.
(42) Huang, S.; Bai, M.; Wang, L. Y. General and Facile Surface Functionalization of Hydrophobic Nanocrystals with Poly(amino acid) for Cell Luminescence Imaging. *Sci. Rep.* **2013**, *3*, 2023−2027.
(43) Ma, Y. X.; Huang, S.; Wang, L. Y. Multifunctional Inorganic−Organic Hybrid Nanospheres for Rapid and Selective Luminescence Detection of TNT in Mixed Nitroaromatics via Magnetic Separation. *Talanta* **2013**, *116*, 535−540.
(44) Salinas, Y.; Martinez-Manez, R.; Jeppesen, J. O.; Petersen, L. H.; Sancenon, F.; Marcos, M. D.; Soto, J.; Guillem, C.; Amoros, P. Tetrathiafulvalene-Capped Hybrid Materials for the Optical Detection of Explosives. *ACS Appl. Mater. Interfaces* **2013**, *5*, 1538−1543.
(45) Dey, N.; Samanta, S. K.; Bhattacharya, S. Selective and Efficient Detection of Nitro-Aromatic Explosives in Multiple Media Including Water, Micelles, Organogel, and Solid Support. *ACS Appl. Mater. Interfaces* **2013**, *5*, 8394−8400.
(46) Vij, V.; Bhalla, V.; Kumar, M. Attogram Detection of Picric Acid by Hexa-peri-Hexabenzocoronene-Based Chemosensors by Controlled Aggregation-Induced Emission Enhancement. *ACS Appl. Mater. Interfaces* **2013**, *5*, 5373−5380.
(47) Xu, S. F.; Lu, H. Z.; Li, J. H.; Song, X. L.; Wang, A. X.; Chen, L. X.; Han, S. B. Dummy Molecularly Imprinted Polymers-Capped CdTe Quantum Dots for the Fluorescent Sensing of 2,4,6-Trinitrotoluene. *ACS Appl. Mater. Interfaces* **2013**, *5*, 8146−8154.